Full Paper: As an example of thermoplastic/liquid crystal blends that do not exhibit a liquid-liquid immiscibility region in their phase diagrams, a polystyrene (PS)/*N*-4-ethoxybenzylidene-4′-butylaniline (EBBA) blend was analyzed. The complete phase diagram was built up using thermal transitions determined by differential scanning calorimetry (DSC) and polarized optical microscopy (POM). The boundary of the nematic + isotropic region was fitted with the Flory-Huggins-Maier-Saupe model, extended to consider the polydispersity of PS. Main factors controlling the morphologies generated by thermal-induced phase separation (TIPS) were the initial EBBA concentration in the blend and the cooling rate. Cooling at a fast rate led to small nematic domains with a narrow size distribution. Slow cooling rates led to the coexistence of very large and small dispersed domains. This was because of the large extent of coalescence of the droplets first generated associated with the continuation of the nucleation/growth process in a medium of increasing viscosity. The use of fast cooling rates might be important for the generation of a narrow size-distribution of nematic droplets by TIPS in polymer-dispersed liquid crystals (PDLC) used in electrooptical devices.

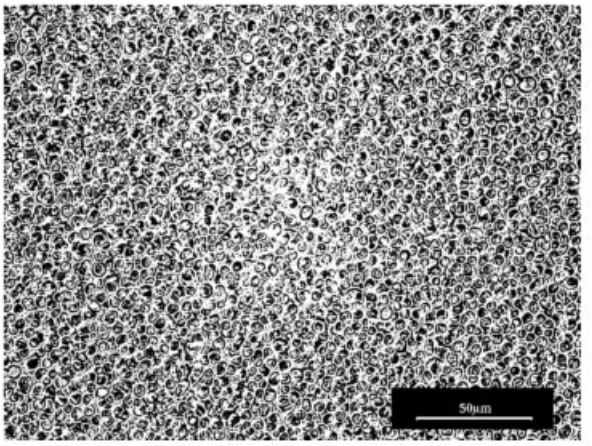

Micrograph obtained by transmission optical microscopy without crossed polarizers, showing nematic domains dispersed in a glassy matrix arising by a fast cooling of the blend from 130 °C; composition of blend: 70 wt.-% EBBA.

Polymer-Dispersed Liquid Crystals Based on Polystyrene and EBBA: Analysis of Phase Diagrams and Morphologies Generated

*Cristina E. Hoppe, María J. Galante, Patricia A. Oyanguren, Roberto J. J. Williams**

Institute of Materials Science and Technology (INTEMA), University of Mar del Plata and National Research Council (CONICET), J. B. Justo 4302, 7600 Mar del Plata, Argentina
Fax: 54 223 481 0046; E-mail: williams@fi.mdp.edu.ar

Keywords: blends; liquid crystals; phase diagrams; phase separation; polystyrene

Introduction

Polymer-dispersed liquid crystals produced by thermal-induced phase separation (TIPS) of a thermoplastic/liquid crystal blend have been the subject of many studies.[1–13] Most of these blends exhibit a liquid-liquid (L-L) immiscibility region in their phase diagrams that precedes the formation of a nematic phase during the cooling step. Therefore, the generated morphologies are determined by the mechanism of the previous L-L phase separation.

Examples of blends that do not exhibit an L-L immiscibility region are the ones of polystyrene (PS) with *N*-4-ethoxybenzylidene-4′-butylaniline (EBBA),[1,3] and of poly(butyl methacrylate) with the nematic mixture E7.[11] These kinds of blends are particularly interesting to study the characteristics of the nematic-isotropic phase separation in a large range of compositions, in the absence of a previous liquid-liquid demixing process. In these cases the formation of nematic domains proceeds through a typical nucleation-growth-coalescence process. An experimental study of one of these blends showed that the average size of dispersed nematic domains increased with the initial liquid crystal concentration and with a decrease in the cooling rate.[11] But to our knowledge, there is no clear answer of how to control the dispersion of particle sizes generated by TIPS, an important question when this type of polymer-dispersed liquid crystals (PDLC) is used in electrooptical devices. A thermoplastic/liquid crystal blend that does not exhibit an L-L immiscibility region is an adequate choice to analyze the

  1022-1352/2003/0705–928$17.50+.50/0

influence of the cooling rate on the generated particle size distribution.

Aims of this study were: a) to build-up the phase diagram of a polydisperse PS-EBBA blend in the whole composition range, including the stability regions of nematic and crystalline phases (previous reported phase diagrams were restricted to the region of low PS concentrations[1] or did not distinguish between nematic and crystalline phases[3]); b) to assess the suitability of the Flory-Huggins-Maier-Saupe (FHMS) model, extended to take polydispersity of the thermoplastic polymer into account[12] to fit the experimental isotropic-nematic curve in a large composition range (the extended model was previously applied to blends exhibiting an L-L immiscibility region in the phase diagram);[12] c) to analyze the influence of the cooling rate on the distribution of the particle sizes.

Experimental Part

Materials

Two different types of polystyrene (PS) were used. The first one was a general purpose PS (Innova HF-555, Monsanto), with a Vicat point of 88 °C. The molar mass distribution was obtained by size exclusion chromatography with PS standards. Average molar masses were $\overline{M}_n = 39\,800$ g/mol, $\overline{M}_w = 297\,000$ g/mol, $\overline{M}_z = 768\,000$ g/mol. The product contains a small amount of added mineral oil to decrease the melt viscosity (and the glass transition temperature). It was subjected to a thermal treatment at 160 °C during 4 h before use. The second PS was a monodisperse product with $\overline{M}_n = 83\,000$ g/mol and $\overline{M}_w = 86\,000$ g/mol (Polymer Source). The polydisperse PS was used in the analysis of both phase diagrams and morphologies generated; the monodisperse PS was employed to analyze the evolution of morphologies during the thermal-induced phase separation.

The liquid crystal, *N*-4-ethoxybenzylidene-4′-butylaniline (EBBA, Aldrich), was used as received. Differential scanning calorimetry (DSC) showed a melting temperature $T_m = 38$ °C and a nematic-isotropic transition temperature $T_{NI} = 77.5$ °C, in agreement with literature values.[1]

Blends of PS and EBBA in the whole range of compositions were prepared by dissolving both components in tetrahydrofuran (THF, 2–15 wt.-%), and heating during 2 h at 130 °C to eliminate the solvent. The more diluted solutions were used to prepare films of about 20 μm thickness for the study of the morphologies.

Techniques

Differential scanning calorimetry (DSC, Pyris 1, Perkin-Elmer) was used to determine thermal transitions during heating scans at 10 °C/min under nitrogen. The samples were first heated to 130 °C, cooled at 10 °C/min to a temperature located below the set of transitions to be measured and heated at 10 °C/min to determine the thermal transitions. The glass transition temperature (T_g) of PS-EBBA solutions was defined as the onset value of the change in the specific heat. The nematic-isotropic transition temperature (T_{NI}) was defined at the end of the characteristic endothermic peak, corresponding to the temperature at which the last fraction of the liquid crystal was dissolved. The resulting T_{NI} is a point located in the isotropic-nematic equilibrium curve, obtained without the undercooling observed when decreasing the temperature from the isotropic region. The melting temperature of EBBA (T_m) was also determined at the end of the characteristic endothermic transition. Heating scans were performed after a storage period of 4–5 days at room temperature to promote crystallization. Several metastable crystal structures are known for EBBA.[14–19] The reported T_m corresponds to the highest temperature at which a crystalline phase could be observed.

Polarized optical microscopy (POM) was employed to determine T_{NI}, defined as the maximum temperature at which nematic domains could be observed between crossed polarizers when heating at 10 °C/min. A Leica DMLB microscope provided with a video camera (Leica DC 100) and a hot stage (Linkam THMS 600), was used for these purposes. Samples were placed between two glass slides using a 0.5 mm stainless steel spacer. Casting of the THF solution was directly performed over one of the glasses, using a spacer to contain the liquid sample. This was followed by evaporation of the solvent during 2 h at 130 °C, placing a glass cover and transferring to the hot stage/microscope at a temperature where the blend was still homogeneous. Then, the sample was heated to 130 °C at 10 °C/min, cooled at the same rate to produce the formation of nematic domains and reheated at 10 °C/min to determine T_{NI}.

The morphologies were observed by optical microscopy with and without crossed polarizers. The blends were prepared from diluted THF solutions (2–5 wt.-%) to give films of about 20 μm thickness. The development of the morphologies was observed in the course of cooling and heating scans at 2 °C/min. The effect of the cooling rate on the generated morphologies was assessed using two different cooling procedures: a) fast cooling: the blends were extracted from the oven at 130 °C and quenched at room temperature; b) slow cooling: the blends were kept in the oven and the temperature was decreased from 130 °C to 25 °C at 0.175 °C/min.

Results and Discussion

Phase Diagram

An illustration of the different thermal transitions observed by DSC in blends of the polydisperse PS with EBBA is shown in Figure 1a–c. The thermal transitions obtained by DSC together with the T_{NI} values determined by POM enabled us to determine the phase diagram of this blend, shown in Figure 2.

The phase diagram shows regions where an isotropic phase is present in either a liquid state (L) or a glassy state (G), and two-phase regions: liquid (L) - nematic (N), liquid (L) - crystal (K), and glass (G) - crystal (K). Nematic and crystal phases are composed by pure EBBA, as results from the application of the thermodynamic model (discussed below). As crystallization is a slow process, the nematic

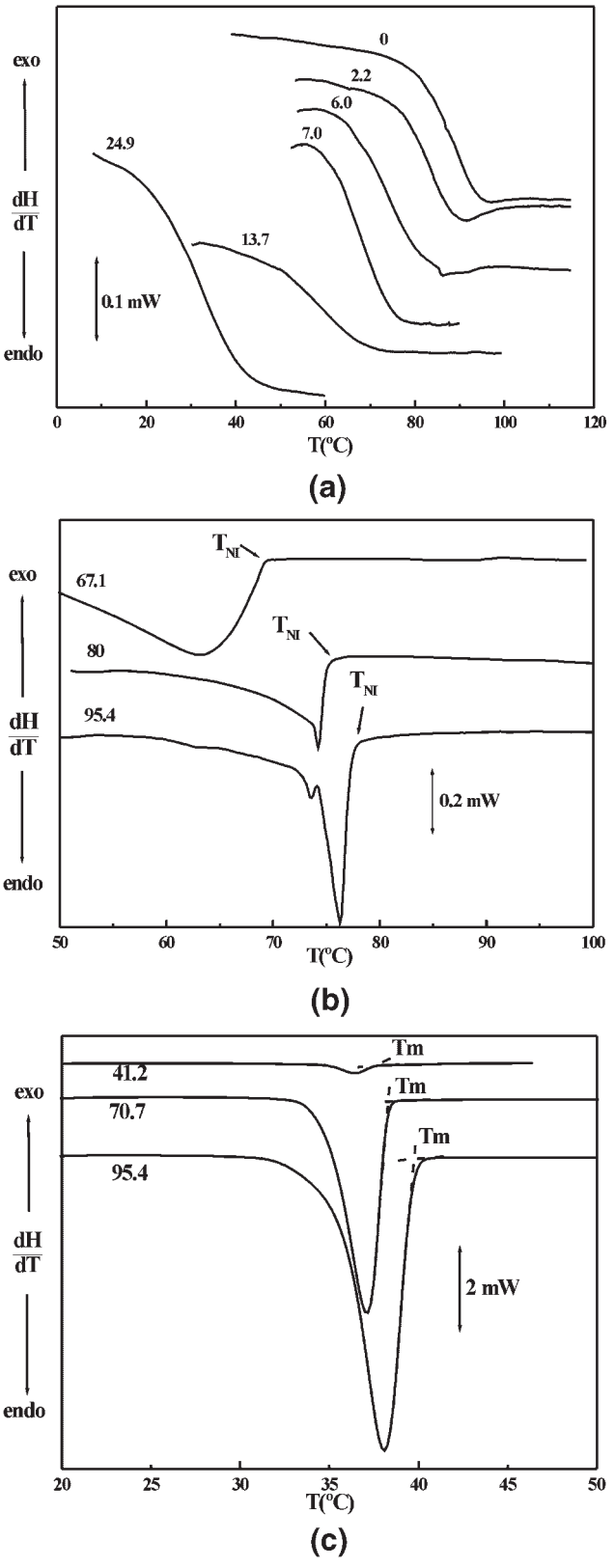

Figure 1. Thermal transitions observed by DSC in blends of the polydisperse PS with EBBA (concentrations are expressed as wt.-% EBBA): a) glass transition temperatures; b) nematic-isotropic transition temperatures; c) melting temperatures.

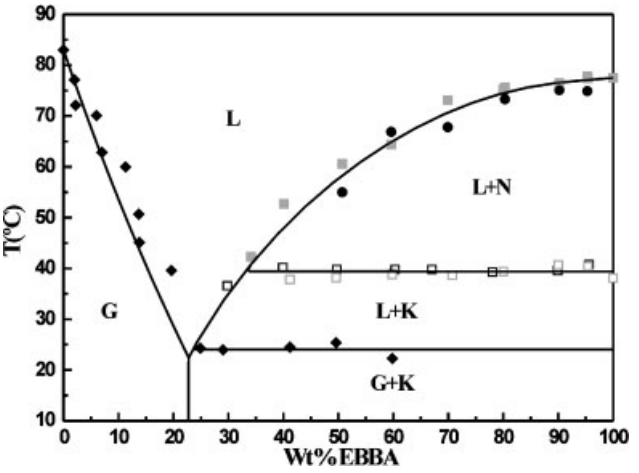

Figure 2. Phase diagram for the polydisperse PS/EBBA blend (T_{NI} values obtained by DSC are indicated with squares while values obtained by POM are denoted with circles).

phase persisted in a metastable condition when cooling down from the L + N region to room temperature. After a few hours at 20 °C, the beginning of crystallization was visually observed and confirmed by DSC.

The crystallization of EBBA at room temperature impedes its use in polymer-dispersed liquid crystals (PDLC) for optical devices. Usually eutectic mixtures of various liquid crystals are used for these purposes, to avoid crystallization and to produce the desired matching of refractive indices. But in any case, the PS/EBBA blend constitutes a model system to analyze the factors that control the morphologies generated.

The solid curve that separates the liquid and glassy states of the isotropic phase represents the variation of the glass transition temperature of the homogeneous blend with composition. It was plotted using the Fox equation:[20]

$$1/T_g = w_{PS}/T_{g,PS} + w_{EBBA}/T_{g,EBBA} \quad (1)$$

where w represents the mass fraction of the particular component. The experimental value of the glass transition temperature of PS was $T_{g,PS} = 356$ K and the corresponding value of EBBA is a virtual value for an isotropic glassy state, which was estimated in a previous publication:[21] $T_{g,EBBA} = 187.3$ K. The Fox equation gave a good fitting of the experimental data, particularly considering that no adjustable parameters were used (the curve was forced to include the experimental point of pure PS but the decrease in T_g when increasing w_{EBBA} was strictly determined by the Fox equation using a literature value for $T_{g,EBBA}$).

The maximum solubility of EBBA in the polydisperse PS is about 23 wt.-%. Blends containing higher mass fractions of EBBA led to a two-phase system when cooling below the equilibrium curve, and produced vitrification of a liquid phase with 23 wt.-% EBBA at $T = 24$ °C. This is the boundary of the G + K region of the phase diagram. During a heating scan from this region, devitrification of the phase

with 23 wt.-% EBBA was observed at 24 °C, followed by the beginning of melting of EBBA crystals. This increased the EBBA concentration in the liquid phase following the equilibrium curve separating the L from the L + K region in the phase diagram. At about 38 °C, the EBBA crystals were completely transformed into a nematic phase. However, for EBBA concentrations in the range 23–33 wt.-%, the final melting of EBBA crystals was observed at a lower temperature along the equilibrium curve (one experimental point in this region is plotted in Figure 2).

When the L + N region was attained during heating, nematic domains began to dissolve at about 38 °C, increasing the EBBA concentration in the liquid phase along the equilibrium curve separating the L from the L + N region. When the equilibrium curve was reached, the nematic domains were completely dissolved leading to an isotropic liquid.

The equilibrium curve separating the L from the L + N regions of the phase diagram was predicted using the Flory-Huggins-Maier-Saupe (FHMS) model,[4,22] extended to consider the polydispersity of PS.[12] In order to apply the model, the molar mass distribution of PS was represented by 50 pseudocomponents (e.g., the continuous distribution was represented by a discrete distribution giving the same average values). The reference volume was taken as the one of the PS repeating unit: $V_r = 99.33$ cm^3. The ratio of average molar volumes of PS with respect to the reference volume were $r_{n,PS} = 382.8$, $r_{w,PS} = 2\,858.6$ and $r_{z,PS} = 7\,388.9$. The ratio of the molar volume of EBBA with respect to the reference volume was $r_{EBBA} = 2.816$. The FHMS model was applied taking the Flory-Huggins interaction parameter $\chi(T)$ as a fitting function. The following expression led to the curve plotted in Figure 2, which shows an excellent agreement with the experimental data:

$$\chi = -0.645 + 287.5/T(\mathrm{K}) \quad (2)$$

For any one of the points of the equilibrium curve, the composition of the segregated phase was practically pure EBBA (predicted mass fractions of EBBA in nematic domains were higher than 99.994%). Therefore, the model predicted that PS was completely segregated from nematic domains.

For consistency purposes, the location of the hypothetical L + L phase region was predicted using the Flory-Huggins model, taking the polydispersity of PS into account as explained above, and using the interaction parameter given by equation (2). The predicted L + L region was located inside the L + N region indicating that two isotropic liquid phases cannot coexist at equilibrium for this particular system.

Morphologies

Blends of the polydisperse PS with EBBA, containing 50, 60, 70 and 80 wt.-% EBBA, were cooled from 130 °C to room temperature, at fast and slow rates, as described in the experimental section. The resulting morphologies were observed by optical microscopy at room temperature before any crystallization took place. The observed morphologies correspond to a dispersion of EBBA domains in a glassy matrix. These domains were in a metastable nematic state at the time where the images were registered.

Figure 3 and 4 show the resulting morphologies obtained with fast and slow cooling rates, respectively. The average size of dispersed domains was estimated using a software for image analysis. As expected, the average size of the nematic domains increased when increasing the initial EBBA content in the blend and with the slow cooling process. The average size of nematic domains for a formulation with 70 wt.-% EBBA increased from 3.5 μm for the fast cooling rate to 13.9 μm for the slow cooling rate (the average size for this case corresponds to the distribution of the large domains). Corresponding values for a blend with 80 wt.-% EBBA were 7.0 μm for the fast cooling rate and 33.7 μm when cooling slowly.

A significant finding was the fact that the distribution of particle sizes was unimodal (nematic domains were distributed in a narrow range of sizes), for fast cooling rates, and bimodal (presence of a distribution of large domains together with another distribution of small domains), for slow cooling rates. When PDLC's are used in electrooptical devices such as reflective displays, optical switches, and variable transmittance windows, it is convenient to generate unimodal distributions of dispersed domains with sizes in the range of the wavelength of visible light.[21] This may be achieved by combining an adequate selection of the initial composition with the use of a fast cooling process.

The different distributions generated with fast and slow cooling procedures may be explained as follows. A fast cooling leads to a high nucleation rate followed by a limited growth/coalescence of dispersed domains. A slow cooling enables a continuous nucleation during the whole cooling process. First nuclei are generated from a solution of low viscosity (high temperatures and an EBBA concentration close to the initial one). This leads to a rapid growth/coalescence process that generates the large nematic domains. But as nucleation continues from solutions of increasing viscosities (at both lower temperatures and EBBA concentrations), the new particles can only evolve limited growth/coalescence processes. This leads to a distribution of very large and small particles (bimodal distributions).

In order to verify this picture, the evolution of morphologies was followed by optical microscopy between crossed polarizers, when cooling at 2 °C/min in the hot stage. As an illustration of these results, Figure 5 shows the evolution of morphologies generated by cooling a blend of the monodisperse PS/EBBA containing 95.3 wt.-% EBBA (although a similar phenomenon was observed with the use of the polydisperse PS, results obtained with the monodisperse PS were selected to avoid speculations

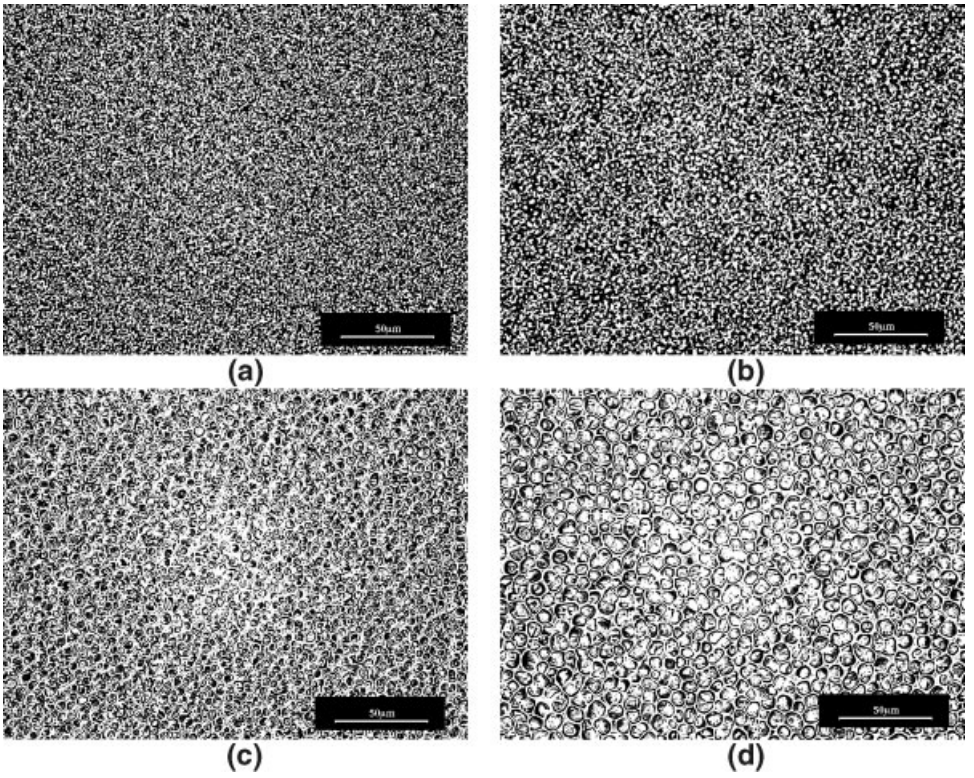

Figure 3. Micrographs obtained by transmission optical microscopy without crossed polarizers, showing nematic domains dispersed in a glassy matrix arising by a fast cooling of blends from 130 °C; composition of blends: a) 50 wt.-% EBBA, b) 60 wt.-% EBBA, c) 70 wt.-% EBBA, d) 80 wt.-% EBBA.

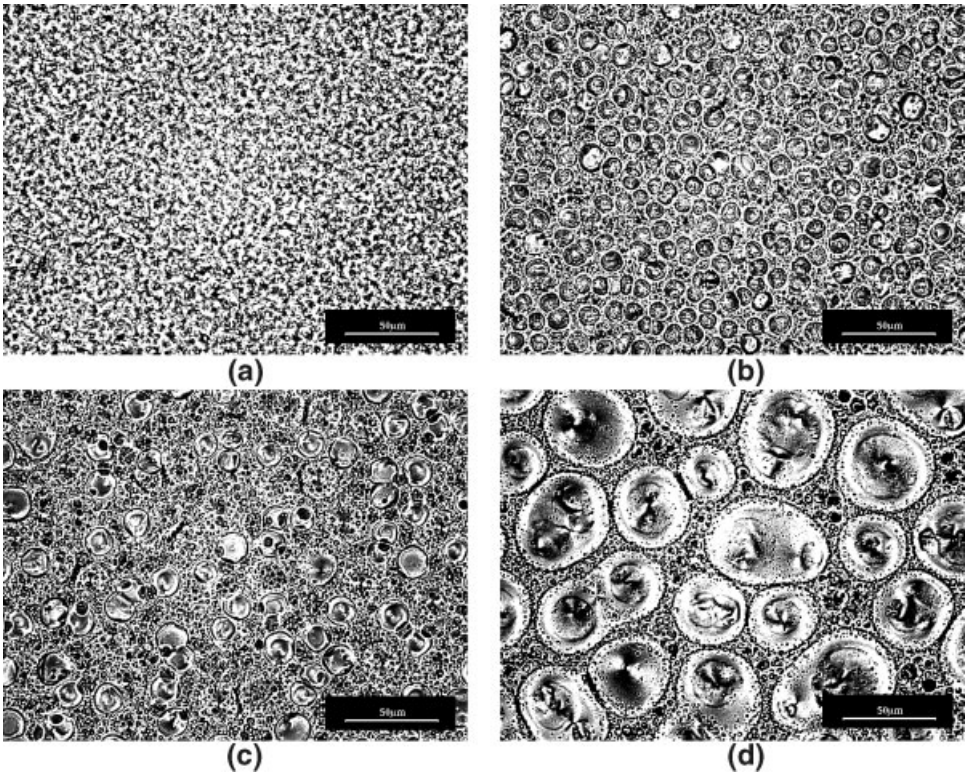

Figure 4. Micrographs obtained by transmission optical microscopy without crossed polarizers, showing nematic domains dispersed in a glassy matrix arising by a slow cooling of blends from 130 °C; composition of blends: a) 50 wt.-% EBBA, b) 60 wt.-% EBBA, c) 70 wt.-% EBBA, d) 80 wt.-% EBBA.

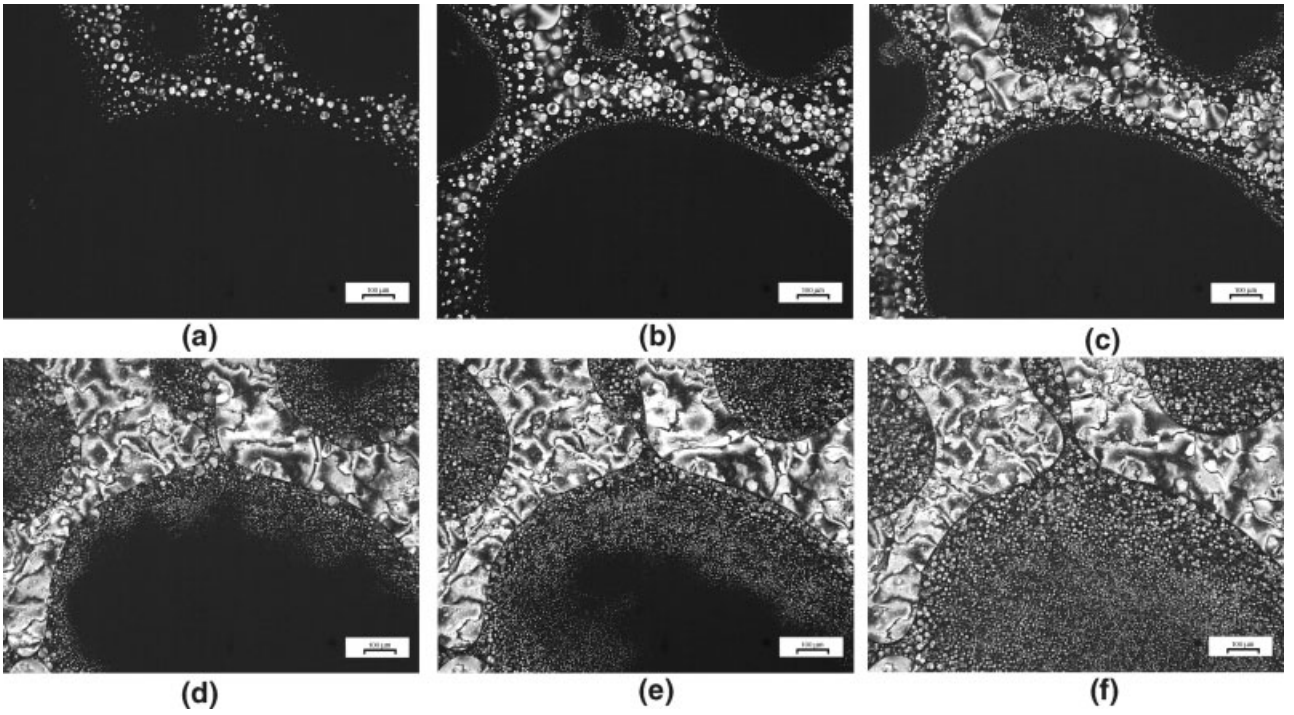

Figure 5. Evolution of morphologies generated by cooling a blend of monodisperse PS/EBBA with 95.3 wt.-% EBBA at 2 °C/min, observed by transmission optical microscopy with crossed polarizers; a) 71.6 °C, b) 71.3 °C, c) 71.0 °C, d) 70.1 °C, e) 69.4 °C, f) 68.4 °C.

regarding the presence of impurities or the fractionation of molar masses).

When cooling from the isotropic liquid phase, the appearance of the first generation of tiny droplets of EBBA was observed at 71.7 °C. At 71.6 °C (Figure 5a), the initial droplets had significantly grown and a new generation of smaller particles was observed (the dark region corresponds to the isotropic PS/EBBA phase). At 71.3 °C (Figure 5b), an agglomeration of the large droplets of nematic domains was observed (initiation of phase inversion). Older particles continued their growth and new particles appeared. When the temperature reached 71.0 °C, the coalescence of the oldest droplets had significantly advanced (Figure 5c). At 70.1 °C (Figure 5d), phase inversion was evidenced by the appearance of a continuous nematic phase leaving dispersed domains of the isotropic solution. As the temperature decreased further (Figure 5e and f), new generations of nematic droplets appeared, covering the whole sample. But they did not merge with the continuous nematic phase possibly because of the high viscosity of the residual isotropic phase, originated by the increase of its PS content and the temperature decrease. A similar process explains the generation of bimodal distributions of nematic domains for blends containing 60–80 wt.-% EBBA, subjected to slow cooling rates. It is important to notice that the final morphology was in fact fixed by the rate at which the system evolved through a temperature region located very close to the isotropic-nematic equilibrium curve.

The evolution of morphologies when heating at 2 °C/min is shown in Figure 6. The smallest droplets are the first to dissolve in the course of heating (Figure 6a and 6b). At 71.6 °C, only some large nematic droplets remain in the interior of the isotropic domains while an incipient thinning of the continuous nematic phase is observed (Figure 6c). A small temperature increase produced a significant thinning (Figure 6d), rupture (Figure 6e), and almost disappearance (Figure 6f) of the nematic phase. Note the slight difference in the temperature of appearance of nematic domains in the cooling cycle (71.7 °C) compared to their disappearance in the heating cycle (73.0 °C). The double peak observed in the DSC heating scan for the nematic-isotropic transition of a blend containing 95.4 wt.-% EBBA (Figure 1b) may be associated to the rapid dissolution of small nematic particles (small peak at lower temperatures), followed by the disappearance of the continuous nematic phase (large peak at higher temperatures).

Conclusions

A complete phase diagram of a PS/EBBA blend was generated as a particular example of thermoplastic/liquid crystal blends that do not exhibit a liquid-liquid demixing region. The boundary of the nematic + isotropic region could be fitted using the Flory-Huggins-Maier-Saupe model, extended to take the polydispersity of PS into account.

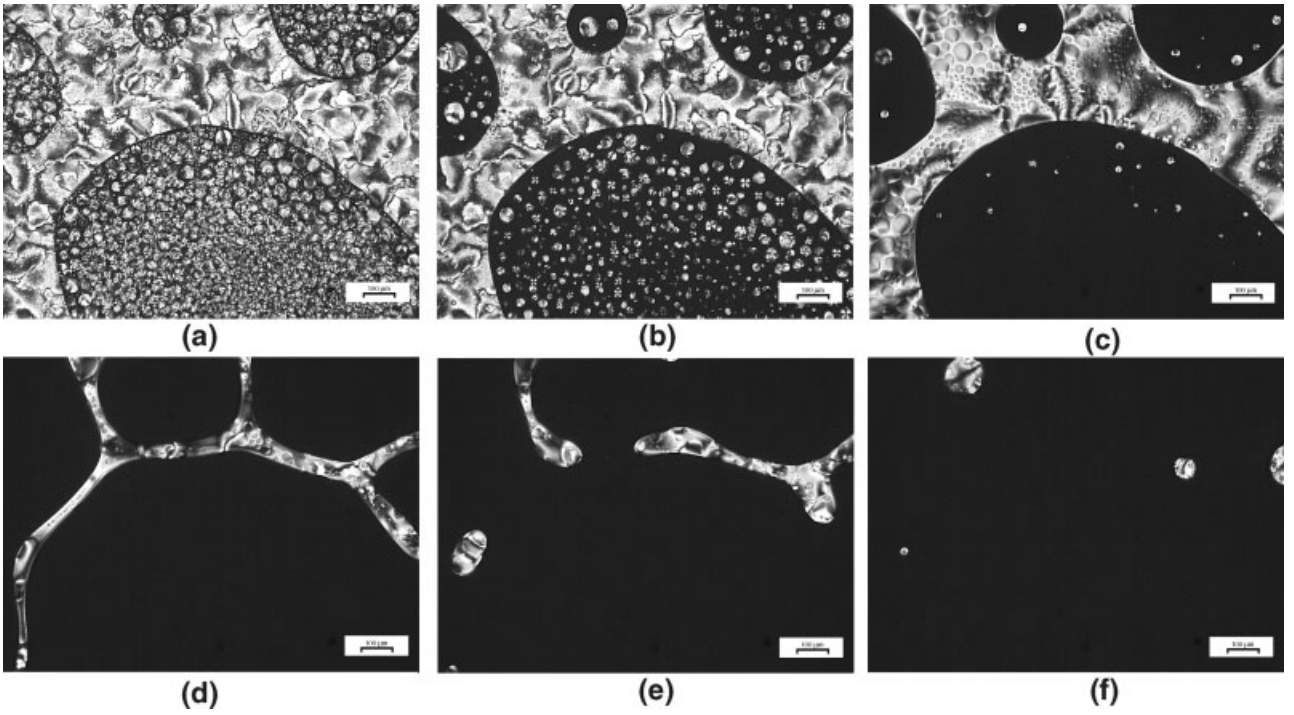

Figure 6. Evolution of morphologies generated by heating a blend of monodisperse PS/EBBA with 95.3 wt.-% EBBA at 2 °C/min, observed by transmission optical microscopy with crossed polarizers; a) 59.4 °C, b) 70.5 °C, c) 71.6 °C, d) 72.3 °C, e) 72.4 °C, f) 72.9 °C.

The model predicted that the composition of the nematic phase was practically pure EBBA, indicating that PS was completely excluded from the nematic domains. The boundary of glassy and liquid states of the isotropic region could be correctly estimated using the Fox equation.

The main factors controlling the morphologies generated were the initial liquid crystal concentration in the blend and the cooling rate. Cooling at a fast rate led to the generation of small nematic domains with a narrow size distribution. Slow cooling rates led to a bimodal particle size distribution with very large and small dispersed domains. The reason therefore was the large extent of coalescence of the droplets first generated and the nucleation of new generations of droplets in a medium of increasing viscosity. The use of fast cooling rates might be important for the generation of a narrow size-distribution of nematic droplets by TIPS in polymer-dispersed liquid crystals (PDLC) used in electrooptical devices.

Acknowledgement: The financial support of the *University of Mar del Plata*, CONICET, ANPCyT, and *Fundación Antorchas* (Argentina), is gratefully acknowledged.

Received: November 2, 2002
Revised: January 11, 2003
Accepted: February 26, 2003

[1] B. Kronberg, I. Bassignana, D. Patterson, *J. Phys. Chem.* **1978**, *82*, 1714.
[2] A. Dubault, C. Casagrande, M. Veyssie, *Mol. Cryst. Liq. Cryst.* **1982**, *72*, 189.
[3] W. Huh, R. A. Weiss, L. Nicolais, *Polym. Eng. Sci.* **1983**, *23*, 779.
[4] V. K. Kelkar, C. Manohar, *Mol. Cryst. Liq. Cryst.* **1986**, *133*, 267.
[5] A. A. Patwardhan, L. A. Belfiore, *Polym. Eng. Sci.* **1988**, *28*, 916.
[6] W. Ahn, C. Y. Kim, H. Kim, S. C. Kim, *Macromolecules* **1992**, *25*, 5002.
[7] T. Kyu, I. Ilies, M. Mustafa, *J. Physique IV* **1993**, *3*, 37.
[8] W. K. Kim, T. Kyu, *Mol. Cryst. Liq. Cryst.* **1994**, *250*, 131.
[9] T. Kyu, I. Ilies, C. Shen, Z. L. Zhou, ''Thermal-Induced Phase Separation in a Mixture of Functional Poly(methyl methacrylate) and Low-Molar-Mass Liquid Crystals'', in: *Liquid Crystalline Polymer Systems*, A. I. Isayev, T. Kyu, S. Z. D. Cheng, Eds., American Chemical Society, Washington DC 1996; *ACS Symp. Ser.* **1996**, *632*, 201.
[10] T. Kyu, C. Shen, H. W. Chiu, *Mol. Cryst. Liq. Cryst.* **1996**, *287*, 27.
[11] L. Carpaneto, A. Ristagno, P. Stagnaro, B. Valenti, *Mol. Cryst. Liq. Cryst.* **1996**, *290*, 213.
[12] C. C. Riccardi, J. Borrajo, R. J. J. Williams, H. Masood Siddiqi, M. Dumon, J. P. Pascault, *Macromolecules* **1998**, *31*, 1124.
[13] F. Roussel, U. Maschke, X. Coqueret, J. M. Buisine, *Mol. Cryst. Liq. Cryst.* **1999**, *329*, 199.
[14] N. Kirov, M. P. Fontana, F. Cavatorta, *J. Mol. Struct.* **1980**, *59*, 147.
[15] N. Kirov, M. P. Fontana, N. Affanassieva, *Mol. Cryst. Liq. Cryst.* **1982**, *89*, 193.

[16] R. Fouret, A. Elouatib, C. Gors, M. More, G. Pepy, L. Rosta, *Phase Transitions* **1991**, *33*, 209.
[17] K. Z. Ogorodnik, S. D. Koshelev, *Sov. Phys. Crystallogr.* **1978**, *23*, 231.
[18] M. Yasuniwa, K. Minato, *Mol. Cryst. Liq. Cryst.* **1982**, *87*, 97.
[19] V. K. Dolganov, M. Gál, N. Kroó, L. Rosta, J. Szabon, *Liq. Cryst.* **1987**, *2*, 73.
[20] T. G. Fox, *Bull. Am. Phys. Soc.* **1956**, *1*, 123.
[21] C. E. Hoppe, M. J. Galante, P. A. Oyanguren, R. J. J. Williams, *Macromolecules* **2002**, *35*, 6324.
[22] C. Shen, T. Kyu, *J. Chem. Phys.* **1995**, *102*, 556.